

## Electrostatic Forces, Molecular-Orbital Theory, and the Electric Field Gradient in Yttrium Iron Garnet

R. M. Housley and R. W. Grant

*North American Rockwell Science Center, Thousand Oaks, California 91360*

(Received 22 May 1972)

We report a Mössbauer determination of  $-0.46$  mm/sec for the electric-quadrupole coupling energy at the octahedral  $\text{Fe}^{3+}$  site in yttrium iron garnet. This and a recently determined value at the tetrahedral  $\text{Fe}^{3+}$  site disagree with the results of a recent linear combination of atomic orbitals-molecular orbital calculation. It is suggested that neglect of the electrostatically produced dipoles on oxygen ions may be the major cause of the disagreement. We suggest a procedure for constructing molecular orbitals taking such dipoles into account.

In the last few years, molecular-orbital theory utilizing linear combinations of atomic orbitals (LCAO) has been applied in a fairly rigorous way to the calculation of electric-field-gradient (EFG) tensor components at nuclear sites in crystals.<sup>1-5</sup> In early tests of the models, the quadrupole moment of  $\text{Al}^{27}$  was deduced from quadrupole resonance data<sup>1-3</sup> in good agreement with an atomic-beam determination, and the quadrupole moment of  $\text{Fe}^{57}$  was determined from Mössbauer data on  $\text{Fe}_2\text{O}_3$ <sup>2,4</sup> and  $\text{FeOCl}$ ,<sup>5</sup> in good agreement with independent results from the analysis of Mössbauer data on ferrous compounds. Recognizing the need for further tests of the models, Sharma and Teng<sup>6</sup> have recently published results calculated from the Sharma<sup>3</sup> model for the EFG at the two crystallographically inequivalent  $\text{Fe}^{3+}$  sites in yttrium iron garnet (YIG).

With these calculations available, it seems worthwhile to obtain as accurate experimental data as possible on the EFG values at the  $\text{Fe}^{3+}$  nuclear sites in YIG. To that end, we have made a Mössbauer study of a YIG single-crystal slab magnetized in the (111) direction. This has allowed us to obtain a room-temperature value of the electric-quadrupole coupling energy  $e^2qQ/2$  at the octahedral  $\text{Fe}^{3+}$  sites with reasonable precision, where  $e$  is the proton charge,  $Q$  the quadrupole moment of  $\text{Fe}^{57}$ , and  $eq$  the element of the diagonalized EFG having the largest magnitude.

The sample in the form of a slab about 6 mm in minimum width and 30  $\mu\text{m}$  in thickness was cut from a flux-grown crystal with a  $\{111\}$  axis normal to the surface. Laue x-ray backscatter techniques were used to verify alignment and quality of the crystal. This sample was mounted in a superconducting magnet with the Dewar constructed in such a way that it remained at room temperature.

Mössbauer data were obtained with an automated, programmed, constant-velocity mechanical drive by using a source of  $\text{Co}^{57}$  in Cu, also at room temperature. A full spectrum is shown in Fig. 1(a); the central region of the spectrum is shown on an expanded velocity scale in Fig. 1(b).

The data were analyzed by first making a least-squares fit of Lorentzian lines to the spectra and then comparing the results with the positions and intensities obtained by diagonalizing the complete interaction Hamiltonian for suitable ranges of hyperfine parameters. In the initial stages of the fitting procedure, constraints were used on some line positions and widths. In the final fit to thirteen lines, all parameters were unconstrained. Calculated linewidths ranged from about 0.25 mm/sec for the inner lines to about 0.35 mm/sec for the outer. Calibration runs with a thin natural Fe foil indicated that the broadening could be largely attributed to instrumental effects. The solid curves through the data in Fig. 1 were calculated from the final least-squares fit.

Above the magnetic-ordering temperature, YIG crystallizes in the cubic space group<sup>7-9</sup>  $Ia\bar{3}d$ ; the unit cell contains 24 crystallographically equivalent  $\text{Y}^{3+}$  ions on dodecahedral  $c$  sites with point symmetry 222, 16 equivalent  $\text{Fe}^{3+}$  ions on octahedral  $a$  sites with point symmetry  $\bar{3}$ , 24 equivalent  $\text{Fe}^{3+}$  ions on tetrahedral  $d$  sites with point symmetry  $\bar{4}$ , and 96 equivalent oxygen ions on sites with identity symmetry. The point symmetry of the  $a$  sites requires the EFG tensor to be axially symmetric and the symmetry axes are equally distributed among the  $\{111\}$  directions. The point symmetry of the  $d$  sites again requires an axially symmetric EFG tensor with the axes in this case evenly distributed among the  $\{100\}$  directions.

With the magnetization along a  $\{111\}$  direction,

the angle  $\theta$  between the EFG symmetry axis and the magnetization is the same for all  $d$  sites and is such that  $\cos^2\theta = \frac{1}{3}$ . This makes the line positions and intensities insensitive to the value of

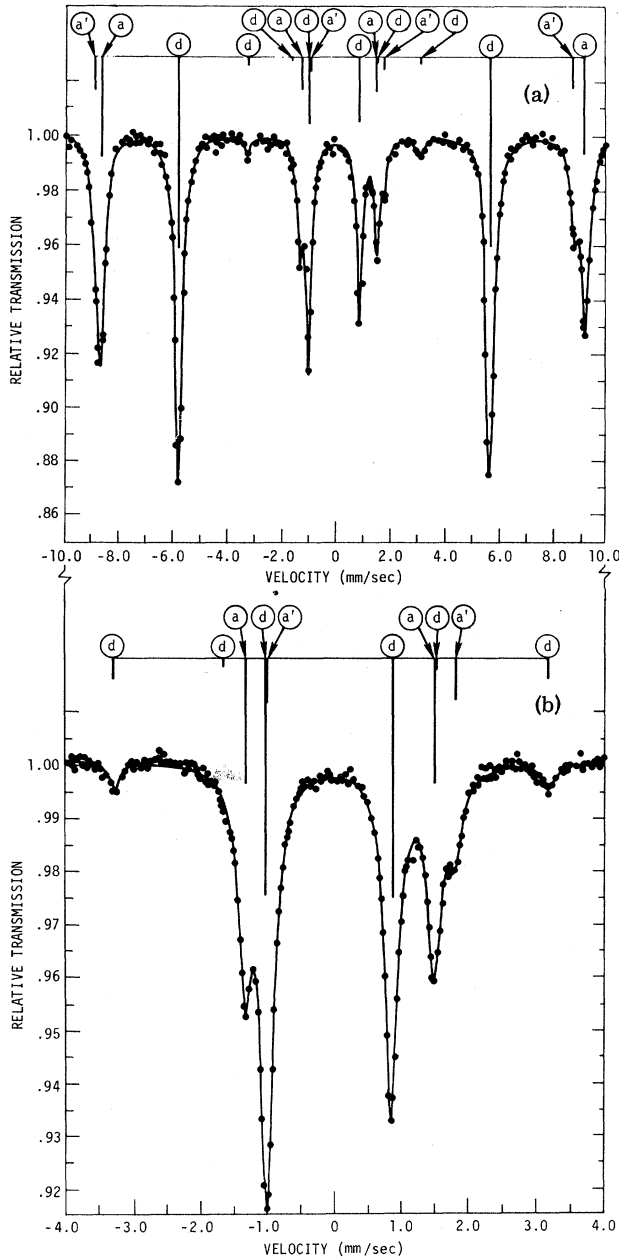


FIG. 1. Mössbauer spectra of a single-crystal 30- $\mu$ m-thick YIG platelet at room temperature obtained with a room-temperature source of  $\text{Co}^{57}$  in Cu. The absorber was in an external magnetic field of 55 kOe directed parallel to the crystallographic (111) direction and the  $\gamma$ -ray propagation direction. The bar diagrams were calculated as described in the text with the letters indicating the sublattice from which lines originate.

the quadrupolar interaction. For four of the  $a$  sites, the corresponding angle is 0, making  $\cos^2\theta = 1$ ; and for the other 12 octahedral sites  $\cos^2\theta = \frac{1}{3}$ . Therefore, the spectra are quite sensitive to the quadrupole interaction at the  $a$  sites.

The line positions and intensities calculated with the set of hyperfine parameters obtained in our final fit are shown by bar diagrams in Figs. 1(a) and 1(b). Of the fourteen lines which are calculated to have observable intensity, with the statistical accuracy of the data, thirteen were resolved in the spectra and these are sufficient to allow an accurate determination of the quadrupole interaction at the octahedral sites. The quadrupole interaction at the tetrahedral site was taken from published data on a crystal magnetized along a  $\{100\}$  direction.<sup>10</sup>

Table I compares the values of the quadrupole interaction at the octahedral and tetrahedral sites calculated by Sharma and Teng<sup>6</sup> with the experimental value for the octahedral site determined in this work and an experimental value for the tetrahedral site recently determined by Belozerskii *et al.*<sup>10</sup> It can be seen that the disagreement is striking, particularly at the octahedral site. Since the disagreement is in the opposite sense at the two sites, it is not possible to obtain agreement by making reasonable changes in the values assumed for  $Q$  or for the antishielding factors.

An apparent shortcoming of the Sharma<sup>3</sup> model is its neglect of electrostatically induced dipole moments on the ligand ions. If such dipole moment values were available, it would be interesting to test the effect of including them as in the Sawatzky-Hupkes<sup>2</sup> model.

Even in the absence of a calculation of the dipole moment on the oxygen ligand sites, it seems important to understand the failure of the Sharma model when applied to YIG in view of its earlier successes in  $\text{Al}_2\text{O}_3$  and  $\text{Fe}_2\text{O}_3$ . In Table II we present data from the literature on the electric field  $E$  at oxygen sites in various oxides, the corresponding induced dipole (assuming an oxygen polarizability of  $2 \text{ \AA}^3$  and neglecting polarization reaction fields), and the displacement of a spherical oxygen  $2p^6$  shell with respect to a spherical core (consisting of the nucleus and the  $1s^2$  and  $2s^2$  electron shells) which would be necessary to produce this dipole moment. Even larger dipole moments have been found in  $\text{BeAl}_2\text{O}_4$ <sup>11</sup> and in various polymorphs of  $\text{Al}_2\text{SiO}_5$ .<sup>12</sup>

From this table it is apparent that  $\text{Al}_2\text{O}_3$  and  $\text{Fe}_2\text{O}_3$  have unusually small electric fields at the

TABLE I. Quadrupole coupling energies at Fe<sup>3+</sup> sites in YIG.

|            | $\frac{1}{2}e^2qQ$ octahedral <i>a</i> site<br>(mm/sec) <sup>a</sup> | $\frac{1}{2}e^2qQ$ tetrahedral <i>d</i> site<br>(mm/sec) <sup>a</sup> |
|------------|--|---|
| Theory     | -1.075 ± 0.098 <sup>b</sup>  | -0.796 ± 0.064 <sup>b</sup>   |
| Experiment | -0.46 ± 0.02 <sup>c</sup>  | -1.03 ± 0.05 <sup>d</sup>   |

<sup>a</sup>To convert to MHz, multiply by 23.4.<sup>b</sup>Ref. 6.<sup>c</sup>This work.<sup>d</sup>Ref. 10.

position of the oxygen sites and hence the electrostatically induced dipoles are unusually small. Since the electrostatic distortion of the oxygen wave functions is small, the probability that the molecular orbitals calculated neglecting that distortion will be good enough to yield results in agreement with experiment is thus maximized for these materials. This also minimizes the difference between the models of Sharma<sup>3</sup> and of Sawatzky and Hupkes.<sup>2</sup>

It seems quite possible that in general for non-cubic sites in ionic materials, electrostatic forces and the corresponding induced dipoles on the anions are so large that direct application of LCAO molecular-orbital theory is inappropriate. In fact, a calculation of such electrostatic forces might be a way of deciding in individual cases whether a standard molecular-orbital treatment was justified or not.

The above line of reasoning leads to the suggestion of a modified procedure for calculating LCAO molecular orbitals for complexes at non-cubic sites in ionic crystals. The shell-model valence-shell displacements would first be cal-

culated using the monopole-self-consistent point-dipole method. The molecular orbitals would then be formed using atomic orbitals for the valence electrons centered on the displaced positions, rather than the nuclear positions.

We wish to thank K. Arita for growing the YIG crystal and K. G. Rasmussen for technical assistance.

<sup>1</sup>D. R. Taylor, *J. Chem. Phys.* **48**, 536 (1968).<sup>2</sup>G. A. Sawatzky and J. Hupkes, *Phys. Rev. Lett.* **25**, 100 (1970).<sup>3</sup>R. R. Sharma, *Phys. Rev. Lett.* **25**, 1622 (1970).<sup>4</sup>R. R. Sharma, *Phys. Rev. Lett.* **26**, 563 (1971).<sup>5</sup>D. Sengupta, J. O. Artman, and G. A. Sawatzky, *Phys. Rev. B* **4**, 1484 (1971).<sup>6</sup>R. R. Sharma and B. N. Teng, *Phys. Rev. Lett.* **27**, 679 (1971).<sup>7</sup>G. Menzer, *Z. Kristallogr., Kristallgeometrie, Kristallphys., Kristallchem.* **69**, 300 (1928).<sup>8</sup>F. Bertaut and F. Forrat, *C. R. Acad. Sci.* **242**, 382 (1956).<sup>9</sup>S. Geller and M. A. Gilleo, *J. Phys. Chem. Solids* **3**, 30 (1957), and **9**, 235 (1959).<sup>10</sup>G. N. Belozerskii, V. N. Gitsovich, A. N. Murin,TABLE II. Electric fields, dipole moments, and shell-model displacements at O<sup>2-</sup> sites in representative oxides.

| Crystal                        | $ E/e $ at oxygen sites <sup>a</sup><br>(Å <sup>-2</sup> ) | Induced dipole <sup>b</sup><br>( $ e \text{Å}$ ) | 2 <i>p</i> shell displacement<br>(Å) |
|--------------------------------|--|--|--------------------------------------|
| Al <sub>2</sub> O <sub>3</sub> | 0.054 <sup>c</sup>   | 0.107  | 0.018                                |
| Cr <sub>2</sub> O <sub>3</sub> | 0.135 <sup>c</sup>   | 0.270  | 0.045                                |
| Ti <sub>2</sub> O <sub>3</sub> | 0.180 <sup>c</sup>   | 0.360  | 0.060                                |
| V <sub>2</sub> O <sub>3</sub>  | 0.134 <sup>c</sup>   | 0.268  | 0.045                                |
| Fe <sub>2</sub> O <sub>3</sub> | 0.014 <sup>d</sup>   | 0.027  | 0.005                                |
| Fe <sub>2</sub> O <sub>3</sub> | 0.013 <sup>e</sup>   | 0.026  | 0.004                                |
| FeOCl                          | 0.173 <sup>f</sup>   | 0.346  | 0.058                                |

<sup>a</sup>Value due to monopoles only. Polarization reaction not included.<sup>b</sup>Assuming an O<sup>2-</sup> polarizability of 2 Å<sup>3</sup>.<sup>c</sup>J. O. Artman, *Phys. Rev.* **143**, 541 (1966).<sup>d</sup>J. O. Artman, A. H. Muir, Jr., and H. Wiedersich, *Phys. Rev.* **173**, 337 (1968).<sup>e</sup>M. Raymond and S. S. Hafner, *Phys. Rev. B* **1**, 979 (1970).<sup>f</sup>R. W. Grant, H. Wiedersich, R. M. Housley, G. P. Espinosa, and J. O. Artman, *Phys. Rev. B* **3**, 678 (1971).

Yu. P. Khimich, and Yu. M. Yakovlev, *Pis'ma Zh. Eksp. Teor. Fiz.* **11**, 173 (1970) [*JETP Lett.* **11**, 106 (1970)], and references to earlier work therein.

<sup>11</sup>L. D. V. Rao and D. V. G. L. N. Rao, *Phys. Rev.* **160**, 274 (1967).

<sup>12</sup>M. Raymond, *Phys. Rev. B* **3**, 3692 (1971).

## Low-Temperature Phase of Infinite Cholesterics\*

T. C. Lubensky

*Physics Department, University of Pennsylvania, Philadelphia, Pennsylvania 19104*

(Received 31 May 1972)

Fluctuations are shown to dephase an infinite cholesteric to a state in which the molecules are aligned preferentially in a plane perpendicular to a pitch axis, but in which all angles in that plane are probed with equal probability. Correlation functions in this state are calculated.

It has been known for some time that infinite two-dimensional systems with a continuous symmetry group cannot exhibit long-range order.<sup>1-3</sup> Nevertheless, high-temperature expansions indicate that there is a phase transition between the isotropic high-temperature and the strongly locally ordered low-temperature phases.<sup>4-6</sup> The nature of the low-temperature phase is now understood, and techniques for calculating correlation functions in this phase exist.<sup>7,8</sup> Recently it was discovered that cholesteric liquid crystals exhibit the same instability with respect to fluctuations in three dimensions that continuous symmetry-group systems exhibit in two dimensions.<sup>9,10</sup> In this Letter, we propose to investigate the properties of the low-temperature phase of an infinite cholesteric. We will rely heavily on the techniques developed by Berezinskii in Ref. 7.

The cholesteric state is characterized by a helical ordering of long barlike molecules. This order is described mathematically by a symmetric traceless tensor whose principal axis rotates in a helical pattern along a pitch axis. To keep the discussion as simple as possible, we will consider a classical spin system with a helical ground state produced by short-range forces as a model for a cholesteric liquid crystal. The spin Hamiltonian we choose is

$$H = -\frac{1}{2} \sum_{\mathbf{r}, \mathbf{r}'} J_{ij}(\mathbf{r} - \mathbf{r}') n_i(\mathbf{r}) n_j(\mathbf{r}'), \quad (1)$$

where

$$J_{ij}(\mathbf{r} - \mathbf{r}') = J(|\mathbf{r} - \mathbf{r}'|) \delta_{ij} - a^{-1} J_1(|\mathbf{r} - \mathbf{r}'|) \epsilon_{ijk} (\mathbf{r} - \mathbf{r}')_k,$$

$a$  is the distance between nearest-neighbor spins, and  $n_i(\mathbf{r}) = (\cos\varphi_2 \cos\varphi, \cos\varphi_2 \sin\varphi, \sin\varphi_2)$ . Equation (1) is represented as a sum over spin sites which can be either at discrete lattice points or continuously distributed in space. The ground state of this Hamiltonian corresponds to a helical ordering of the classical spins,

$$n_i^0(\mathbf{r}) = (\cos q_0 z, \sin q_0 z, 0), \quad (2)$$

with energy

$$E_0 = -\frac{1}{2} N [J(q_0) - a^{-1} J_1'(q_0)],$$

where

$$J(q_0) = \sum_{\mathbf{r}} J(|\mathbf{r}|) \exp(i\vec{q}_0 \cdot \mathbf{r})$$

and  $q_0$  satisfies

$$J'(q_0) - a^{-1} J_1''(q_0) = 0.$$

$z$  is along an arbitrarily chosen pitch axis  $\vec{p}$  ( $\vec{p}$  is a unit vector). An expansion of Eq. (1) in terms of the gradients of  $n_i(\mathbf{r})$  yields an expression equivalent to the Frank free energy with equal elastic constants.<sup>11</sup> Correlation functions for small deviations from this ground state have been calculated in